Online Peak Detection in Photoplethysmogram Signals Using Sequential Learning Algorithm

B. N. Sumukha
PES Centre for Int. Sys.
PES University Campus
Bangalore, India.
sumukha.bn@gmail.com

R. Chandan Kumar
PES Centre for Int. Sys.
PES University Campus
Bangalore, India.
chandanrkumar619@gmail.com

Skanda S. Bharadwaj
PES Centre for Int. Sys.
PES University Campus
Bangalore, India.
Skandabharadwaj94@gmail.com

Koshy George
PES Centre for Int. Sys.;
Dept. of Tel. Engg., PESIT
Bangalore, India.
kgeorge@pes.edu

***Abstract*—Photoplethysmogram signals are becoming increasingly important for the detection of abnormalities in patients. Peak detection plays a significant role in diagnosis and monitoring using PPG signals. Although a copious number of methods are available for peak detection, none of them consider an online processing of the signal. In this paper we propose an online peak detection algorithm that tries to mimic the human cognitive model using a three-layered feedforward neural network trained using online sequential learning algorithm. The signals are processed sequentially without pre-processing or feature extraction, and result in an almost instantaneous detection of peaks.**

I. Introduction

Photoplethysmogram (PPG) is an optically obtained signal that provides information about the changes in the blood volume in the micro-vascular tissue bed. These signals are recorded by placing electrodes on the skin surface of peripheral body sites such as finger and ear-lobe. The PPG signal is useful for monitoring heart rate, cardiac cycles, respiration, depth of anaesthesia, and hypo- and hyper-volemia. Parameters like pulse transmit time and pulse wave velocity obtained from the systolic peaks of the PPG signal are used in determining important parameters pertaining to the health of a patient; these include blood pressure [1], stiffness of the arteries [2], left ventricular ejection time, left ventricular pre-ejection period [3], and blood in surgical operation [4]. The objective of this paper is to propose a novel technique to detect and locate the peaks in a PPG signal.

Whilst a number of researchers have dealt with Electrocardiogram (ECG) signal analysis and QRS complex detection, there appears to be very little work on the peak detection of PPG signals. QRS complex detection is based on the impulsive nature of the signal. In contrast, PPG signals — as can be observed from Fig. 1 — has characteristics that bear resemblance to a sinusoidal signal. In this paper, we exploit this to arrive at a peak detection technique.

There are a variety of methods to detect peaks. These include the conventional window threshold technique [5], [6]; the use of transforms such as wavelet or Hilbert transforms [7], [8]; Kalman or nonlinear filtering [9], [10]; and, hidden Markov models [11]. In [12], the author iteratively determines the autocorrelation sequence to detect regions of interest and thresholds to detect peaks. By adapting the segment lengths and comparing maximum points of consecutive segments

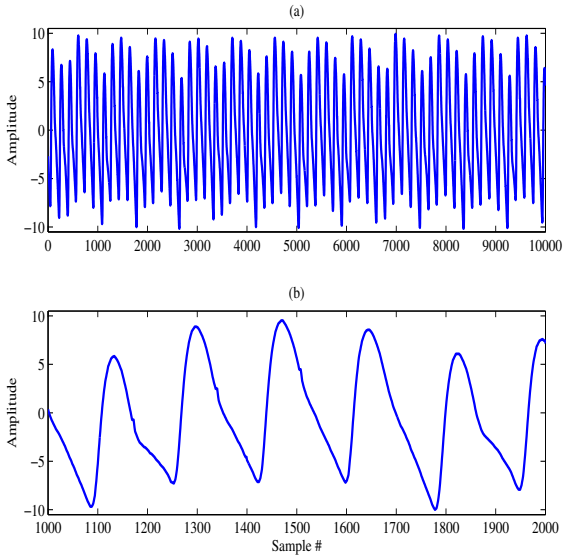

Fig. 1. A sample photoplethysmogram signal.

peaks of PPG signals are detected in [13]. Artificial neural networks were used in [14] and [15], and clustering techniques in [16]. The authors in [17] present an automatic multiscale-based peak detection algorithm.

Thus, despite a profusion of algorithms, they typically involve pre-processing and feature extraction, and hence computationally rather intensive. Moreover, a fundamental requirement for these algorithms is the availability of the entire signal. Accordingly, these methods consider offline training with the available data. As seen later in the sequel, the proposed algorithm avoids these requirements, is online in nature, and is quite intuitive. From a practical viewpoint, online learning is better suited for real-time applications. Our focus is on developing tools and hand-held devices that provide assessment of the health of a patient with minimal energy usage. Requirements for this include online processing of signals and algorithms that are computationally less expensive.

In this paper, we present a methodology for detecting the peaks in a signal by first classifying segments of the signal into a set of fundamental a priori defined classes. Only

978-1-5090-6182-2/17/$31.00 ©2017 IEEE

those segments that contain a peak are further processed to detect and determine the precise location of the peaks. The classification is carried out using a feedforward neural network (FFNN) that is trained using an online sequential learning algorithm (OSLA). The classification process avoids complex pre-processing and feature extraction.

The paper is organised as follows: In Section II we discuss the methodology. The algorithm used to train the FFNN is presented in Section III. Results on two classes of signals are provided in Section IV.

II. Peak Detection Methodology

The proposed technique for detecting peaks is essentially based on recognising the shape of the graph of a function or signal. (In what follows, this is referred to as the 'shape of a signal.') In this section, we first describe the method with the family of signals represented by a finite sum of sinusoids. Subsequently, we extend the idea to PPG signals, and finally present a simplified approach for these signals.

Essentially, we exploit the human cognitive process which does not require the entire signal to be available a priori to detect and locate a peak. In contrast to conventional methods, it is able to detect a peak as and when portions of the signal are shown. In our context, we employ online classification of segments of a signal and detect the peaks nearly instantaneously. Such an approach appears to be novel to the authors' best knowledge.

A. Peak Detection in Sinusoidal Signals Using Fundamental Classes Drawn from Sinusoids (PDSS)

Commonly occurring signals in nature are periodic. It is well-known that these can either be represented by a finite sum of sinusoids with different frequencies and phases, or approximated by such a finite sum. A sinusoidal signal has essentially four shapes as shown in Fig. 2; we refer to them as the fundamental classes. Class 1 represents the graph wherein the gradient of the graph is nonnegative and Class 2 represents the graph wherein the gradient is initially nonnegative and subsequently nonpositive. Signals belonging to Classes 3 and 4 respectively are merely the reflections about the x-axis of signals belonging to Classes 1 and 2, respectively.

Obviously, only Class 2 contains a peak, and requires further processing to locate the peak. The classes 1 through 4 are respectively denoted $\mathcal{C}_1$, $\mathcal{C}_2$, $\mathcal{C}_3$ and $\mathcal{C}_4$. Thus, the principal idea is to first classify segments of a given signal as belonging to one of the four classes, $\mathcal{C}_1$, $\mathcal{C}_2$, $\mathcal{C}_3$ or $\mathcal{C}_4$. Subsequently, only those segments belonging to $\mathcal{C}_2$ are further processed to detect the location of the peak. Evidently, the efficiency of peak detection algorithm is strongly related to the classification accuracy.

Consider the following family of signals

$$S = \left\{ s(t) : s(t) = \sum_{i=0}^{m} \sin \omega_i t, \quad \omega_i \in \mathbb{R}_+, \quad m \in \mathbb{N} \right\} \quad (1)$$

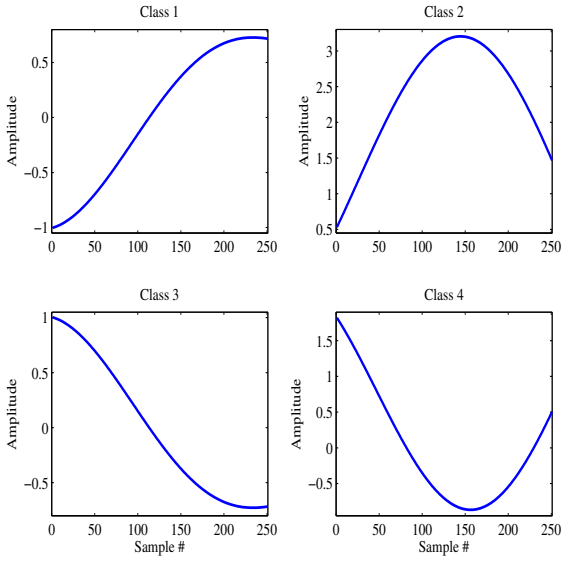

Fig. 2. Fundamental classes of a sinusoidal signal.

where $\mathbb{R}_+$ is the set of strictly positive real numbers and $\mathbb{N}$ is the set of natural numbers. For any $s(t) \in S$, let

$$s_p(t) = \begin{cases} s(t), & t \in [t_1, t_2] \\ 0, & \text{otherwise} \end{cases} \quad (2)$$

be a segment of $s(t)$. Clearly, for suitably chosen t_1 and t_2, the shape of $s_p(t)$ belong to one of the $\mathcal{C}_i$s. A segmented portion being classified as belonging to $\mathcal{C}_2$ is equivalent to detecting a peak. Thus, peak detection and location in a signal belonging to S is achieved by first classifying non-overlapping segments into the four fundamental classes that are derived from a sinusoid; we refer to this as PDSS.

The method to automatically choose t_1 and t_2 in (2) is not clear a priori. In this paper, we experimentally choose as follows the segment length $L = t_2 - t_1$ which gives the best classification accuracy: A heuristic is provided by the Nyquist criteria. The chosen database consists of signals sampled with a frequency of 450 Hz; accordingly, an approximate value of L is one-fourth of this sampling frequency, namely, 112. Further experimentation reveals that a window length of 101 provides acceptable results. Evidently, such experimentation is restricted to the data required to train the artificial neural network.

A feedforward neural network is trained to recognise the four fundamental classes. For faster training and classification we use a network with a single hidden layer and a sequential learning algorithm presented in Section III. The raw signals are shown to the network; i.e., we avoid complex pre-processing and feature extraction. Once the network is trained, an entire signal $s(t) \in S$ is presented to the network with the samples shown sequentially. If a segment (or a window) of suitably chosen length L is classified as $\mathcal{C}_2$, it is further considered for peak detection; the latter is merely obtaining the maximum of

the samples present in that particular window, and determining its location. The simulation results are presented in Section IV. The proposed method for peak detection is clearly on-line and intuitive, and does not require offline complex pre-processing and feature extraction.

The manner in which the segments are processed indicates that more than one segment containing the same peak is likely to be classified as belonging to $\mathcal{C}_2$. This can result in an increase of the peak count. In order to mitigate such spurious peak detection, the central position of the segment is monitored. Only those segments are considered for peak location and count wherein the maximum value in a particular segment is located at the central position.

B. Peak Detection in PPG Signals Using Fundamental Classes Drawn from PPG Signals (PDPP)

As evident from Fig. 1, PPG signals are much more complicated than sinusoids. Therefore, peak detection in these signals is not as straightforward as that of sinusoidal signals. Nonetheless, the idea presented earlier for sinusoidal signals works as well for PPG signals.

In this paper, we consider the PPG signals available from the IEEE TBME Respiratory Rate Benchmark data set associated with [18]. The number of available signals is 42. In our work we consider the raw signals and we do not consider pre-processing. The signals are partitioned into segments of length L. Clearly, the choice of the value of L depends on the signals. As mentioned earlier, a heuristic is provided by the Nyquist criteria. Since the sampling frequency is 300 Hz, an initial guess of the window length is 75. Further experimentation reveals that $L = 81$ provides acceptable results. The four fundamental shapes for PPG signals are shown in Fig. 3. Only Class 2 is considered to contain a peak. Thus, we use these four fundamental shapes derived from a PPG signal to classify segments of PPG signals to determine whether or not there is a peak; we refer to this as PDPP.

As evident from Fig. 3, effective gradient determination is not as straightforward as in the case of sinusoids as the graphs are not sufficiently smooth. To train the neural network we require class labels for each segment. Towards this, the first step is to obtain a piecewise linear approximation from the samples. (This makes the signal smoother to some extent and is an attempt to avoid spurious peaks.) The effective slope is derived from the slopes of the individual slopes of the linear approximations which are either nonpositive or nonnegative. The effective slopes of the first and second halves of the segment determine the class label. Similar to PDSS, we train a three-layered FFNN with OSLA to classify using these class labels.

C. Peak Detection in PPG Signals Using Fundamental Classes Drawn from Sinusoidal Signals (PDPS)

From a human visual standpoint, a peak of a signal is merely the highest point of a segment of the corresponding graph. Accordingly, at a certain depth of vision, the second fundamental shape of a PPG signal shown in Fig. 3 bears a close resemblance to a signal belonging to $\mathcal{C}_2$ shown in Fig. 2. In this section, we exploit this resemblance to detect the peaks in a PPG signal. In other words, we use the fundamental classes $\mathcal{C}_1$ through $\mathcal{C}_4$ derived from the sinusoid to classify segments of a PPG signal; we refer to this as PDPS.

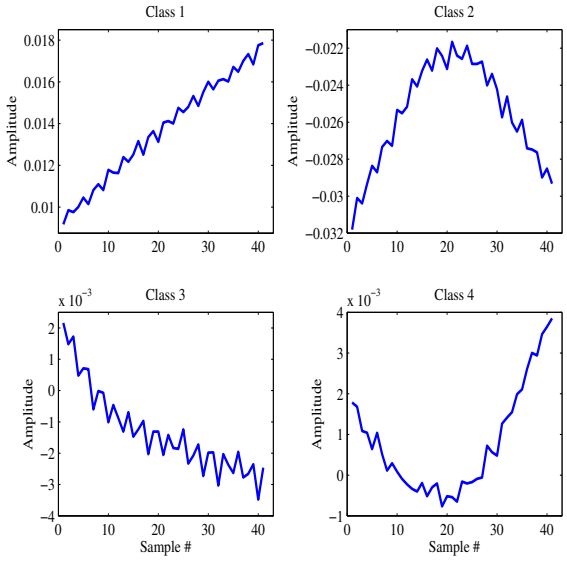

Fig. 3. Fundamental shapes of a PPG signal.

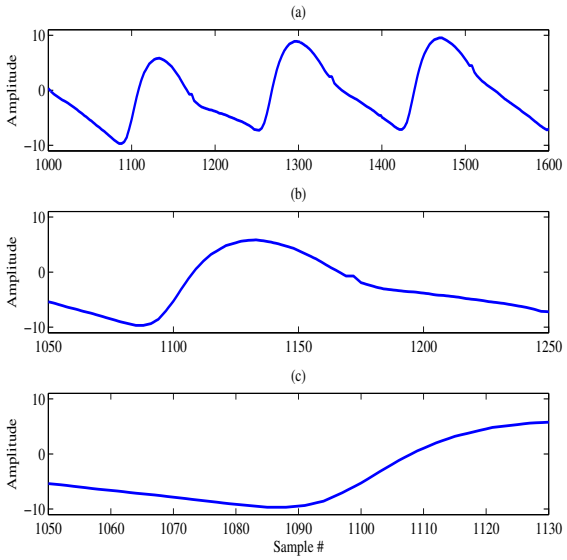

Fig. 4. Visualization of depth of a signal while perceiving it with different window lengths. The depth is largest in (a) and it is myopic in (c). A satisfactory depth is given in (b).

The depth of vision can be quantified in terms of the length of a segment. The effect of this length is illustrated in Fig. 4. A larger length increases the depth of vision and encompasses more than one peak; this is shown in Fig. 4(a). This makes the peak detection process more complex. In contrast, a myopic vision as depicted in Fig. 4(c) leads to a situation wherein the

peak is not detected. However, if the length of the window is chosen appropriately, a single peak can be observed as evident from Fig. 4(b), and closely resembles $\mathcal{C}_2$. Thus, with a proper segment length, classification of segments of a very different signal such as PPG can be carried out using the classifier of PDSS. We recall that the segment length for PDSS was experimentally found to be 101. For PDPS, this is the apt window length.

III. Online Sequential Learning Algorithm

In this paper we consider three-layered feedforward neural networks (FFNN) with m_0 input nodes, m_1 neurons in the hidden layer and m_2 output neurons. We denote such a network as $\mathcal{N}_{m_0:m_1:m_2}$. Whilst the hidden layer is nonlinear with the activation function $\phi(v) = \tanh(v)$, the output layer is linear with unity gain. The set of synaptic weights that connect the input nodes to the hidden layer can be arranged as an array, denoted W_1. Similarly, the synaptic weights that connect the hidden layer to the output layer is a matrix denoted W_2. From the equations that follow it is obvious that W_1 and W_2 have dimensions $m_1 \times (m_0+1)$ and $m_2 \times (m_1+1)$, where the bias has also been taken into account.

The ordered pairs of data are denoted $(\mathbf{x}_k, \mathbf{y}_{d,k})$, where $\mathbf{x}_k \in \mathbb{R}^{m_0}$ and $\mathbf{y}_{d,k} \in \mathbb{R}^{m_2}$, and k indicates the sample number. Here, $\mathbf{x}_k$ is the input to the network and $\mathbf{y}_{d,k}$ is the desired output of the network. The computations in the forward pass may be summarised as follows:

$$\bar{\mathbf{y}}_{1,k} = \phi\left(W_1 \mathbf{y}_{0,k}\right) \quad (3)$$

$$\mathbf{y}_{2,k} = W_2 \mathbf{y}_{1,k} \quad (4)$$

where

$$\mathbf{y}_{0,k} \triangleq \begin{pmatrix} 1 \\ \mathbf{x}_k \end{pmatrix}, \quad \mathbf{y}_{1,k} \triangleq \begin{pmatrix} 1 \\ \bar{\mathbf{y}}_k \end{pmatrix}.$$

In the online sequential learning algorithm (OSLA), the weight matrix W_1 is initialised randomly and the weight matrix W_2 is set to a zero matrix. Subsequently, the weight matrix W_2 is updated as follows: For $k \geq 0$,

$$P_{k+1} = P_k - \frac{P_k \mathbf{y}_{1,k+1} \mathbf{y}_{1,k+1}^T P_k}{1 + \mathbf{y}_{1,k+1}^T P_k \mathbf{y}_{1,k+1}} \quad (5)$$

$$W_{2,k+1} = W_{2,k} + \mathbf{e}_{k+1} \mathbf{y}_{1,k+1}^T P_{k+1} \quad (6)$$

where the error in the a priori estimate

$$\mathbf{e}_{k+1} \triangleq \mathbf{y}_{d,k+1} - W_{2,k} \mathbf{y}_{1,k+1}$$

and $P_0 = \frac{1}{\lambda} I_{m_1+1}$ with I_m an identity matrix of dimensions $m \times m$ and $\lambda > 0$. Note that the weight matrix W_1 is not updated.

It is quite straightforward to show that the update equations (5) and (6) correspond to the recursive least squares solution to the Tikhonov-Phillips functional

$$J = \|W_2 Y_1 - Y_d\| + \lambda \|W_2\|, \quad (7)$$

where λ is also known as the regularisation parameter ([19]–[21]), and

$$Y_1 = \begin{pmatrix} \mathbf{y}_{1,1} & \mathbf{y}_{1,2} & \cdots & \mathbf{y}_{1,N} \end{pmatrix}$$

$$Y_d = \begin{pmatrix} \mathbf{y}_{d,1} & \mathbf{y}_{d,2} & \cdots & \mathbf{y}_{d,N} \end{pmatrix}$$

Here, it is assumed that the data consists of N pairs of input and output. The parameter λ provides a trade-off between minimisation of the training error and the synaptic weights of the output layer. Clearly, the minimiser of (7) is global.

Comments: (i) In contrast to the back propagation algorithm, the OSLA converges to the global minimum. Experience indicates that the convergence of OSLA is faster. It may be noted, however, that the back propagation algorithm is applicable to FFNNs with arbitrary number of hidden layers. (ii) The weight update equations (5) and (6) are similar to the weight update equations of the online sequential extreme learning machine (OSELM) proposed in [22], the sequential version of the extreme learning machine [23]. However, in contrast to OSELM, the initialisations are quite different. The different initialisation of OSLA results in much better performance compared to other sequential forms of learning including OSELM in the context of system identification and control [24], [25] and time-series prediction [26].

IV. Results and Discussions

The first set of experiments consists of detecting and locating the peaks of signals in S using the four fundamental classes that are extracted from sinusoids and shown in Fig. 2; i.e., we now present the results related to PDSS described in Section II-A. The chosen window length is 101. Therefore, we consider a FFNN with $m_0 = 101$ input nodes. Further, the number of neurons in the output layer is $m_2 = 4$ since there are four classes. The number of hidden neurons m_1 is experimentally chosen to be 400 based on achieved classification accuracy. (We denote this network as $\mathcal{N}^{(1)}_{101:400:4}$.) The training set consists of 918, 1092, 908 and 1072 segments respectively belonging to the classes $\mathcal{C}_1$, $\mathcal{C}_2$, $\mathcal{C}_3$ and $\mathcal{C}_4$. The percentages of correct classification are respectively 95.5, 98.1, 95.4 and 98.5.

The confusion matrix for the training data is shown in Fig. 5. It may be recalled that the only class of interest from the viewpoint of peak detection is $\mathcal{C}_2$. Of the 1092 segments that belong to this class, 1071 segments have been correctly classified resulting in a percentage accuracy of 98.1; 10 of the segments have been wrongly classified as class $\mathcal{C}_1$; and, 11 of the segments have been wrongly classified as class $\mathcal{C}_3$. There are a total of 3990 segments. Accordingly, the percentage of segments correctly classified as $\mathcal{C}_2$ is 26.8. Similarly, 10 of the total number of segments have been wrongly classified as $\mathcal{C}_1$ resulting in an approximate percentage of 0.3; and, so on. These facts correspond to the second row of the confusion matrix in Fig. 5. In addition to 1071 segments correctly classified, 27 segments that belong to $\mathcal{C}_1$ have been wrongly classified as $\mathcal{C}_2$, and 20 segments that belong to $\mathcal{C}_3$ have been wrongly classified as $\mathcal{C}_2$. Thus, there are 1118 segments that

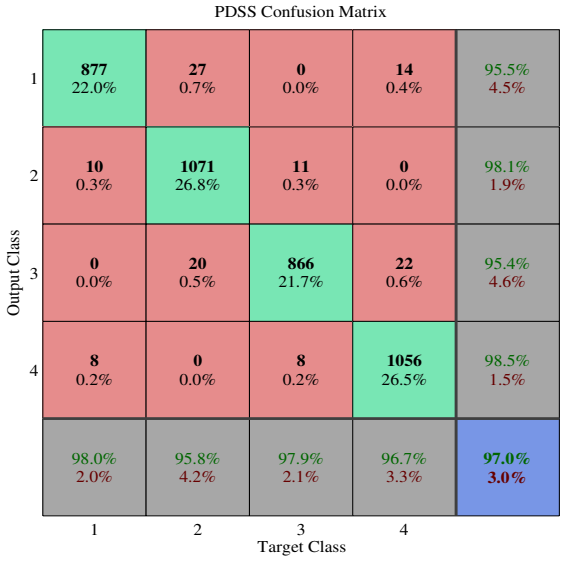

Fig. 5. Confusion matrix related to classification of signals in S based on the four fundamental classes; i.e., PDSS.

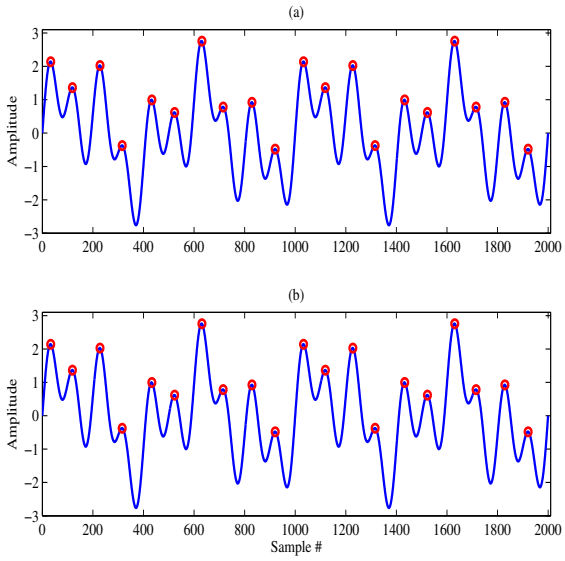

Fig. 6. Results of peak detection in a sinusoidal signal. (a) Using the built-in function findpeaks. (b) Using the proposed algorithm PDSS.

have been classified as $\mathcal{C}_2$. Of these only 1071 are correctly classified; this corresponds to 95.8%. This is shown as the 2nd entry of the last row. Amongst all classes, there are a total of 3870 segments correctly classified; this corresponds to 97% of the total number of segments 3990, and is the overall accuracy of the classification process. This is the last entry of the last row in the confusion matrix.

Those segments that belong to class $\mathcal{C}_2$ are then passed on to the peak detector and processed as explained in Section II-A. These results of peak detection are shown in Fig. 6(a) and compared with those obtained by using the findpeaks function of MATLAB which are shown in Fig. 6(b). Evidently, there is no difference between the two methods. To quantify this, the accuracy of detection of peaks in sinusoidal signals with PDSS is calculated with respect to the output of findpeaks; that is, the peak detection accuracy (PDA) is the ratio

$$\text{PDA}_{\text{PDSS}} = \frac{\text{Number of peaks detected by PDSS}}{\text{Number of peaks detected by findpeaks}} \qquad (8)$$

expressed as a percentage. For PDSS, the PDA is observed to be 100%. Thus, it can easily be seen that the proposed technique performs rather well. It may be noted that the database consists of noise-free signals and hence the peak detection process using either method is quite straightforward.

Comments: Essentially, the MATLAB function findpeaks compares neighbouring points and determines all those peaks that are separated by a minimum distance, and larger than their neighbours by a threshold. Clearly, this function requires the a priori availability of the complete signal, and is offline in nature.

For the experiments related to PDPP and described in Section II-B, a second feedforward neural network is trained using the fundamental shapes extracted from the PPG signals

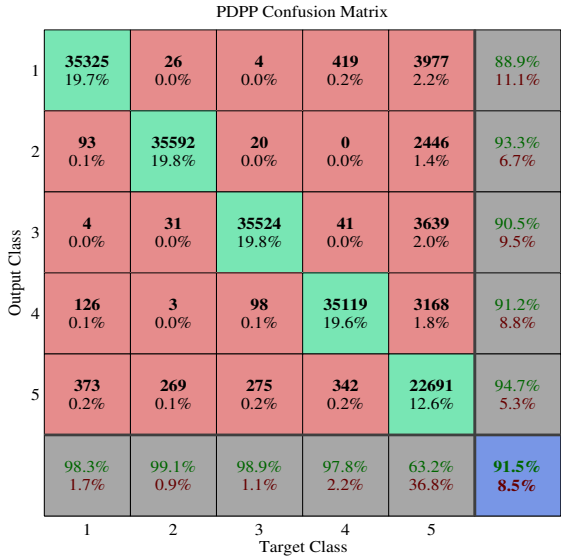

Fig. 7. Confusion matrix related to classification of PPG signals based on the four fundamental shapes; i.e., PDPP.

and shown in Fig. 3. As explained in Section II-B, the window length that provides the best classification accuracy is 81. Moreover, the number of hidden neurons is experimentally chosen to be 400. Thus, for this network, $m_0 = 81$, $m_1 = 400$, and $m_2 = 5$. (We denote this network as $\mathcal{N}^{(2)}_{81:400:5}$.) Since the PPG signals are not as smooth as the previous database of sum of sinusoids, we add a fifth class which consists of segments that are anomalous in that they do not reasonably resemble any of the four fundamental classes. This class is essentially a set of segments that are to be discarded.

The confusion matrix for segments of PPG classified from

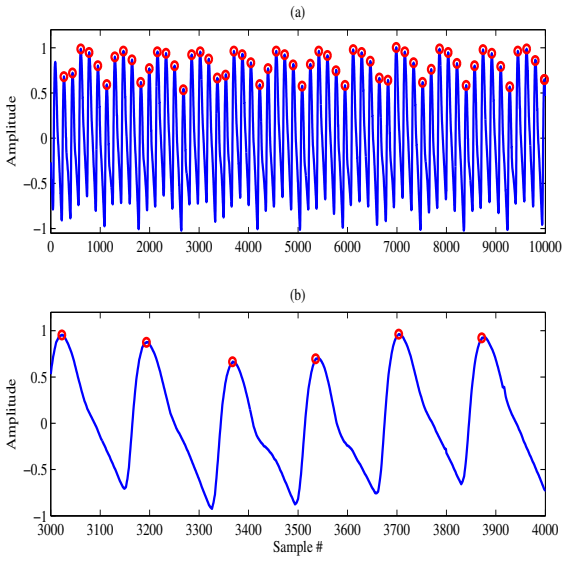

Fig. 8. Results of peak detection in a PPG signal using the proposed algorithm PDPP. The results are zoomed in (b).

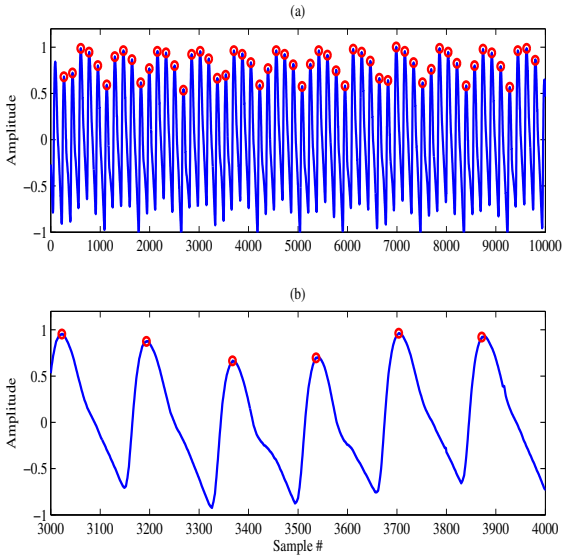

Fig. 9. Results of peak detection in a PPG signal using the proposed algorithm PDPS. The results are zoomed in (b).

the four fundamental shapes extracted from PPG signals is provided in Fig. 7. (The explanation of this confusion matrix is similar to that for the confusion matrix shown in Fig. 5.) The overall classification accuracy is 91.5%. However, the only class of interest is $\mathcal{C}_2$ for which the classification accuracy is 93.3%. The results of peak detection is shown in Fig. 8. A magnified version is shown in Fig. 8(b). Evidently, the proposed algorithm performs satisfactorily. However, not all the peaks are detected. Indeed the value of the metric PDA as determined from (8) (with PDSS replaced by PDPP) is 91.38%, averaged over all the signals in the database.

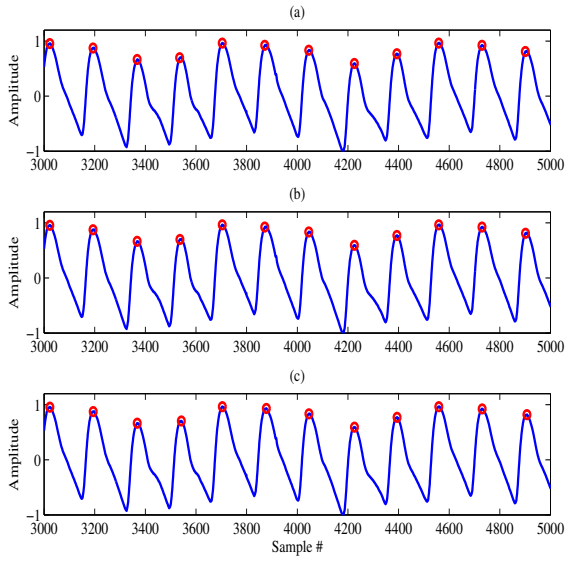

Fig. 10. Results of peak detection in a PPG signal using (a) PDPP, (b) PDPS, and (c) findpeaks.

Finally, we detect the peaks in the PPG signal using the fundamental classes derived from the sinusoidal signal; i.e., we use the method PDPS described in Section II-C. We emphasise that we use the same trained network $\mathcal{N}^{(1)}_{101:400:4}$ that was used to classify segments of sinusoidal signals into the four fundamental classes $\mathcal{C}_1$ through $\mathcal{C}_4$. Accordingly, there is no additional training and the network is tested on the set of PPG signals that this network has not been exposed to a priori. Clearly, the window length that is used now is 101. This window length helps to visualise the signal from a particular depth where it is perceived to be closer to a sinusoid. The results of peak detection is observed to be satisfactory from Fig. 9.

The three methods — PDPP, PDPS, and findpeaks — to detect peaks in a PPG signal are compared in Figures 10 and 11. The latter figure indicates that the proposed methods do not always detect the peaks. Evidently, the proposed methods PDPP and PDPS provide results that are comparable to the MATLAB built-in function findpeaks. The value of the metric PDA as determined from (8) (with PDSS replaced by PDPS) is 97.93%, averaged over all the signals in the database. (The total number of signals in the database is 42.) Evidently, PDPS provides significantly better detection accuracy when compared to PDPP. We note that classification in PDPS did not require additional training of the network; the network that was trained to classify segments of sinusoidal segments was used directly on the database of PPG signals.

We now present statistical analysis based on the Wilcoxon signed rank test. We first compare the classification of segments using the online sequential learning algorithm with that of a neural network trained with the back propagation algorithm. For a 5% significance level, the null hypothesis failed with a p-value of 0.04. Accordingly, the median of the

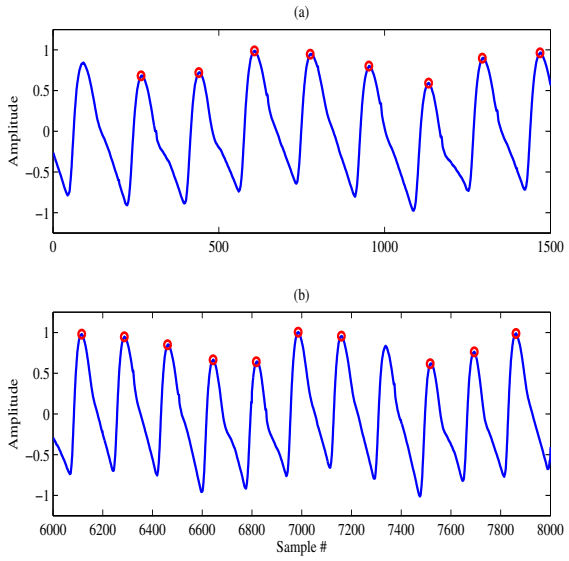

Fig. 11. Results of peak detection in a PPG signal using (a) PDPP, and (b) PDPS.

distributions corresponding to the algorithms are significantly different. Indeed, it has been the experience that OSLA provides better classification accuracies. However, the test failed to reject the null hypothesis when the three methods for peak detection — PDSS, PDPP and PDPS — are compared with the results of findpeaks for the 5% significance level. The respective p-values are 0.8649, 0.8773 and 0.6557. Therefore, there is no significant difference between the proposed methods for peak detection and the findpeaks algorithm. However, in the context of peak detection of PPG signals, it was observed that PDPS performed better in terms of the metric PDA.

V. Conclusions

In this paper we presented a methodology for detecting the peaks of a noisy complex signal such as PPG using principles derived from the human cognitive process. Essentially, when viewed from the proper depth, segments of the signal resemble the fundamental classes of a sinusoidal signal. Moreover, the human cognitive process is online and sequential. Accordingly, the methodology consists of classifying segments of a signal, and subsequently locates and detects the peak of only those segments that contain a peak. The classification uses a three-layered network trained with the online sequential learning algorithm. No complex pre-processing of signals and feature extraction are required for the classification process during training as well as testing. The classification is therefore online and sequential. Thus, peak detection can be carried out on-the-fly. The results are comparable with an often-used conventional peak detection algorithm. Work is in progress to statistically compare this algorithm with multiple datasets and different algorithms.

References

[1] H. Gesche, D. Grosskurth, G. Kuchler, and A. Patzak, "Continuous blood pressure measurement by using the pulse transit time: comparison to a cuff-based method," *European Journal of Applied Physiology*, vol. 112, no. 1, pp. 309–315, 2012.

[2] J. Y. A. Foo, S. J. Williams, G. Williams, M. A. Harris, and D. Cooper, "Pulse transit time as a derived non invasive mean to monitor arterial distensibility changes in children," *Journal of Human Hypertension*, vol. 19, pp. 723–729, 2005.

[3] J. Allen, "Photoplethysmography and its application in clinical physiological measurement," *Physiological Measurement*, vol. 28, no. 3, pp. R1–R39, March 2007.

[4] C. H. Wang, C. W. Lu, T. Y. Lin, M. F. Abbod, and J. S. Shieh, "An assessment of pulse transit time for detecting heavy blood loss during surgical operation," *The Open Biomedical Engineering Journal*, vol. 6, pp. 104–111, 2012.

[5] A. L. Jacobsen, "Auto-threshold peak detection in physiological signals," in *Proceedings of the 23rd Annual Conference of the IEEE*, vol. 3, Al-Ain, UAE, 2001, pp. 2194–2195.

[6] J. Pan and W. J. Tompkins, "A real-time QRS detection algorithm," *IEEE Transactions on Biomedical Engineering*, vol. 32, pp. 230–236, March 1985.

[7] P. Du, W. A. Kibbe, and S. M. Lin, "Improved peak detection in mass spectrum by incorporating continuous wavelet transform-based pattern matching," *Bioinformatics*, vol. 22, no. 17, pp. 2059–2065, August 2006.

[8] D. Benitez, P. A. Gaydecki, A. Zaidi, and A. P. Fitzpatrick, "The use of the Hilbert transform in ECG signal analysis," *Computers in Biology and Medicine*, vol. 31, no. 5, pp. 399–406, September 2001.

[9] M. Aboy, J. McNames, T. Thong, D. Tsunami, M. S. Ellenby, and B. Goldstein, "An automatic beat detection algorithm for pressure signals," *IEEE Transactions on Biomedical Engineering*, vol. 52, no. 10, pp. 1662–1670, October 2005.

[10] A. T. Tzallas, V. P. Oikonomou, and D. I. Fotiadis, "Epileptic spike detection using a kalman filter based approach," in *Proceedings of the 28th IEEE EMBS Annual International Conference*, New York, NY, USA, August-September 2006, pp. 501–504.

[11] D. A. Coast, R. M. Stern, G. G. Cano, and S. A. Briller, "An approach to cardiac arrhythmia analysis using hidden markov models," *IEEE Transactions on Biomedical Engineering*, vol. 37, no. 6, pp. 826–836, September 1990.

[12] D. P. A. Kilgour, S. Hughes, S. L. Kilgour, C. L. Mackay, M. Palmblad, B. Q. Tran, Y. A. Goo, R. K. Ernst, D. J. Clarke, and D. R. Goodlett, "Autopiquer — a robust and reliable peak detection algorithm for mass spectrometry," *Journal of the American Society for Mass Spectrometry*, vol. 28, no. 2, pp. 253–262, February 2017.

[13] A. R. Kavsaoğlu, K. Polat, and M. R. Bozkurt, "An innovation peak detection algorithm for photoplethysmography signals: an adaptive segmentation method," *Turkish Journal of Electrical Engineering & Computer Sciences*, vol. 24, pp. 1782–1796, 2016.

[14] Q. Xue, Y. H. Hu, and W. J. Tompkins, "Neural-network-based adaptive matched filtering for QRS detection," *IEEE Transanctions on Biomedical Engineering*, vol. 39, no. 4, pp. 317–329, April 1992.

[15] G. Vijaya, V. Kumar, and H. K. Verma, "ANN-based QRS-complex analysis of ECG," *Journal of Medical Engineering and Technology*, vol. 22, no. 4, pp. 160–167, 1998.

[16] S. S. Mehta, D. A. Shete, N. S. Lingayat, and V. S. Chouhan, "K-means algorithm for the detection and delineation of QRS-complexes in electrocardiogram," *IRBM*, vol. 31, no. 1, pp. 48–54, February 2010.

[17] F. Scholkmann, J. Boss, and M. Wolf, "An efficient algorithm for automatic peak detection in noisy periodic and quasi-periodic signals," *Algorithms*, vol. 5, pp. 588–603, December 2012.

[18] W. Karlen, S. Raman, J. M. Ansermino, and G. A. Dumont, "Multiparameter respiratory rate estimation from the photoplethysmogram," *IEEE Transactions on Biomedical Engineering*, vol. 60, pp. 1946–1953, July 2013, www.capnobase.org/database/pulse-oximeter-ieee-tbme-benchmark/.

[19] D. Phillips, "A technique for the numerical solution of certain integral equations of the first kind," *Journal of Association for Computing Machinery*, vol. 9, pp. 84–97, 1962.

[20] A. N. Tikhonov, "On solving incorrectly posed problems and method of regularization," *Doklady Akademii Nauk USSR*, vol. 151, pp. 501–504, 1963.

[21] A. N. Tikhonov and V. Y. Arsenin, *Solutions of Ill-Posed Problems*. Washington, DC, USA: V. H. Winston & Sons, 1977.

[22] N.-Y. Liang, G.-B. Huang, P. Saratchandran, and N. Sundararajan, "A fast and accurate online sequential learning algorithm for feedforward networks," *IEEE Transactions on Neural Networks*, vol. 17, pp. 1411–1423, 2006.

[23] G.-B. Huang, Q.-Y. Zhu, and C.-K. Siew, "Extreme learning machine: Theory and applications," *Neurocomputing*, vol. 70, pp. 489–501, 2006.

[24] K. Subramanian, S. G. Krishnappa, and K. George, "Performance comparison of learning algorithms for system identification and control," in *Proceedings of the 12th IEEE India International Conference (INDICON 2015)*, New Delhi, India, December 2015.

[25] K. George, K. Subramanian, and N. Seshadhri, "Improving transient performance in adaptive control of nonlinear systems," in *Proceedings of the 4th International Conference on Advances in Control and Optimization of Dynamical Systems (ACODS16)*, Tiruchirappali, India, February 2016, pp. 658–663.

[26] K. George and P. Mutalik, "Online time series prediction with metacognition," in *Proceedings of the International Joint Conference on Neural Networks (IJCNN 2016)*, Vancouver, BC, Canada, July 2016.